2014 American Control Conference (ACC)
June 4-6, 2014. Portland, Oregon, USA

Modeling, Simulation and Control of a Seamless Two-Speed Automated Transmission for Electric Vehicles*

Mir Saman Rahimi Mousavi and Benoit Boulet, *Senior Member*, *IEEE*

***Abstract*— Power transfer and gear shifting control are the main duties of the transmission in a vehicle. This paper focuses on the modeling, simulation and control of a two speed automated transmission for electric vehicles having a seamless gear shifting specification. The transmission incorporates two-stage planetary gear sets and two braking mechanisms to control the gear shifting. Controlling the input power of the electric motor and the embedded brakes provides seamless flow of power during a gear change. The dynamic model of the mechanism has been developed by using the power and the kinematic equations of the planetary gear trains and the free body diagram of the mechanism. The simulation model has been built up in MATLAB/*Simulink*® to investigate the performance of the proposed controller. The control algorithm is inspired by the two main control phases in Dual Clutch Transmissions (DCT), namely the torque phase and the inertia phase. An Input Output Feedback Linearization control technique with a PID controller are used for the torque phase and an optimal MIMO H_∞ controller is designed for the inertia phase. Simulation results show the ability of the proposed transmission with the control algorithm to have a smooth gear change without excessive oscillations in the output torque and speed.**

I. INTRODUCTION

Increasing fuel cost and environmental concerns have pushed the automotive industry to gradually replace internal combustion engine (ICE) vehicles with hybrid electric (HEV) and fully electric (EV) vehicles. However, the energy density of electric batteries is much less than that of fossil fuels. So, it is needed to optimize the efficiency of the driveline to maximize the range of HEVs and EVs. An important component of the driveline, which plays a crucial role on fuel consumption and comfort, is the transmission [1, 2]. The transmission provides speed and torque conversion from the powertrain to the driveline. The two main common transmissions are automatic (AT) and manual (MT). The ATs are easier than MTs to use but they consume more fuel than MTs. The MTs give the driver more control on the speed of the vehicle but they are less convenient than ATs. Much research has been conducted to find the best solution with the benefits of both AT and MT transmissions. Continuously Variable (CVT), Automated Manual (AMT) and Dual Clutch Transmissions (DCT) are the most famous ones [3, 4, 5].

The dynamic analysis and control of the CVT are studied in [6, 7]. The optimization problem for fuel consumption and efficiency are solved in [8, 9]. In [1, 10] the model of the driveline, the dry clutch and the hydraulic actuators for an AMT transmission are presented. Thereafter, the different working phases of the AMT are discussed and the controllers for each phase are designed and validated. In [11], a dynamic sliding-mode controller with adaptive tuning for controlling the clutch of the AMT transmission is presented. The controller is validated by experimental tests. In [12, 13, 14], the modeling of a driveline equipped with DCT is presented. In the DCT transmissions, the clutch-to-clutch torque transfer should be done smoothly to increase the driveability of the vehicle. This torque transfer is performed by two different phases called the torque phase and the inertia phase. In [12], a closed-loop control algorithm for both the upshift and downshift and a suitable sequence of these two phases was presented and validated by simulation. One of the main differences between AMT and DCT transmissions is that in the AMT, during gear shifting, the driveline is disengaged and re-engaged to the powertrain which reduces passenger comfort and lifetime of the synchronizer. However, in the DCT, the power is always transferred through the clutch surfaces. In this paper, a two-speed automated transmission for electric vehicles is proposed. This system is similar to the DCT in its behaviour but mechanically different. The proposed transmission is comprised of a dual stage planetary gearbox with common ring and common sun. The ratio of the pitch diameter of the ring to the sun in the input and output sides are different in order to have two different gear ratios. Two friction brakes are used to control the flow of power during gearshift to have a fast and smooth gear change. These two friction brakes control the speed of the sun and the ring gears. Fig. 1 shows the schematic view of the proposed transmission.

According to Fig. 1, the input of the transmission is the carrier on the left hand side of the figure, which is attached to a Permanent Magnet Synchronized Motor (PMSM). The output of the mechanism is the carrier on the right hand side which is attached to the load. Two different gear ratios can be obtained by fixing the sun or the ring. Furthermore, by controlling the brakes, the gear shifting can be made seamless and without any torque interruption. Fig. 2 shows the expansion view of the 3D CAD model of the transmission. In this paper, for the brevity, sun, ring and planets are used instead of sun gear, ring gear and planet gears, respectively.

II. KINEMATIC ANALYSIS OF THE PROPOSED TRANSMISSION

A. Kinematic Equations

As the planetary gear trains are the main components of the proposed transmission, the required kinematic equations

*This work was supported by Automotive Partnership Canada (APC).

M.S Rahimi Mousavi and B. Boulet are with the Department of Electrical Engineering, McGill University, Montréal, QC H3A 2T5, Canada, saman@cim.mcgill.ca.

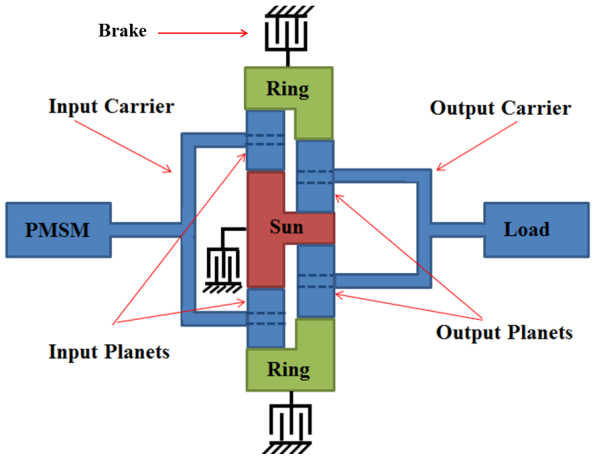

Fig. 1. Schematic view of the Two Speed Automated Transmission

to derive the equations of motion are reviewed. The kinematic equations between a planetary gear component such as Carrier (C), Sun(S), Planets (P) and Ring (R) are as follows [15]:

$$r_R\omega_R = r_P\omega_P + r_C\omega_C;\ r_R = r_P + r_C \tag{1}$$

$$r_C\omega_C = r_P\omega_P + r_S\omega_S;\ r_C = r_P + r_S \tag{2}$$

Where r_S, r_P and r_R are the pitch radius of sun, planet and ring, respectively. The parameter r_C is the radius of the circle on which the planets are mounted. The parameters ω_S, ω_P, ω_R and ω_C are the angular velocity of the sun, planets, ring and carrier, respectively. By eliminating ω_P and r_P from equations (1) and (2), the kinematic relation between the Ring, Sun and Carrier is as follows:

$$(r_R + r_S)\omega_C = r_S\omega_S + r_R\omega_R \tag{3}$$

For simplification of the formulation, the ratio of the pitch radius of the ring $r_{p,R}$ to the sun $r_{p,S}$ in the input and the output of the transmission are considered as:

$$R_1 := \left(\frac{r_{p,R}}{r_{p,S}}\right)_{input} \tag{4}$$

$$R_2 := \left(\frac{r_{p,R}}{r_{p,S}}\right)_{output} \tag{5}$$

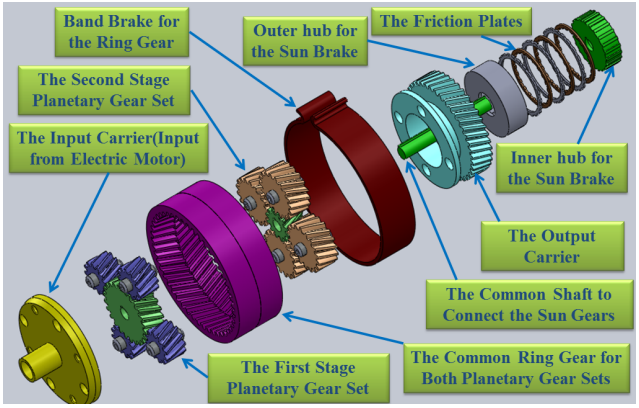

Fig. 2. Expansion view of the Two-Speed Automated Transmission

It is obvious that R_1 and R_2 are greater than one because the pitch radius of the ring is always greater than the sun's.

Now, by considering $(\omega_C)_{input} = \omega_{in,T}$ and $(\omega_C)_{output} = \omega_{out,T}$, where $(\omega_C)_{input}$ is the angular speed of the input carrier and $(\omega_C)_{output}$ is the angular speed of output carrier, the equations (3)-(5) can be written as:

$$\omega_{in,T}(R_1 + 1) = \omega_S + R_1\omega_R \tag{6}$$

$$\omega_{out,T}(R_2 + 1) = \omega_S + R_2\omega_R \tag{7}$$

Equations (6) and (7) are the main kinematic equations of the system which will be used to derive the equations of motion.

B. Gear Ratios

In this section, the achievable gear ratios of the system will be discussed. According to equations (6) and (7), the speed ratio of the input of the transmission to the output can be expressed as follows:

$$\frac{\omega_{in,T}}{\omega_{out,T}} = \frac{(R_2 + 1)(\omega_S + R_1\omega_R)}{(R_1 + 1)(\omega_S + R_2\omega_R)} \tag{8}$$

According to equation (8), three different gear ratios are achievable:

1) If the ring is completely grounded ($\omega_R = 0$):

$$\frac{\omega_{in,T}}{\omega_{out,T}} = \frac{(R_2 + 1)}{(R_1 + 1)} = GR_1 \tag{9}$$

2) If the sun is completely grounded ($\omega_S = 0$):

$$\frac{\omega_{in,T}}{\omega_{out,T}} = \frac{(R_2 + 1)R_1}{(R_1 + 1)R_2} = GR_2 \tag{10}$$

3) If neither sun nor ring are completely grounded ($\omega_R \neq 0$ and $\omega_S \neq 0$):

$$\frac{\omega_{in,T}}{\omega_{out,T}} = \frac{(R_2 + 1)(\omega_S + R_1\omega_R)}{(R_1 + 1)(\omega_S + R_2\omega_R)} = GR_T \tag{11}$$

If both sun and ring gears are grounded, the system will be locked. Here, GR_1 and GR_2 are considered as the first and the second gear ratios where GR_T is the transient gear ratio from the first gear ratio to the second one during gear shifting. Even though the gear ratios are dependent, it is possible to solve the equations (9) and (10) for R_1 and R_2 to get the desired GR_1 and GR_2.

III. DYNAMIC EQUATIONS

In this section, the dynamic equations of the system are presented for control purposes.

Firstly, the power equation of the system is pointed out. Here, it is assumed that the power loss is just caused by the two embedded brakes of the transmission. Hence, the input power will be distributed on the ring and sun without any loss and the output power of the system equals to the summation of output power of ring and sun. So:

$$\begin{cases} P_{in,T} = P_{in,R} + P_{in,S} \\ P_{out,T} = P_{out,R} + P_{out,S} \end{cases} \tag{12}$$

Where $P_{in,T}$ is the input power which comes from the electric motor. $P_{in,R}$ and $P_{in,S}$ are the power transferred to the ring and the sun from the input side of the transmission. $P_{out,T}$ is the power which goes out of the transmission to the load. $P_{out,R}$ and $P_{out,S}$ are the power transferred from the ring and sun to the output of the transmission. The output power of the transmission could be less than the input power when the transmission is in GR_T mode. This happens when $\omega_R \neq 0$ and $\omega_S \neq 0$.

Here, the mechanical power is calculated as the product of the angular velocity and the torque ($P = T\omega$). Hence, according to equation (12):

$$\begin{cases} T_{in,T}\,\omega_{in,T} = T_{in,R}\,\omega_R + T_{in,S}\,\omega_S \\ T_{out,T}\,\omega_{out,T} = T_{out,R}\,\omega_R + T_{out,S}\,\omega_S \end{cases} \tag{13}$$

Where $T_{in,R}$ and $T_{in,S}$ are the torques applied to the ring and the sun from the input carrier and $T_{out,R}$ and $T_{out,S}$ are the torques applied from the load to the ring and the sun.

From equations (6),(7),(12) and (13) it can be easily concluded that:

$$\begin{cases} T_{in,R} = \dfrac{T_{in,T}R_1}{R_1+1}, \quad T_{out,R} = \dfrac{T_{out,T}R_2}{R_2+1} \\ T_{in,S} = \dfrac{T_{in,T}}{R_1+1}, \quad T_{out,S} = \dfrac{T_{out,T}}{R_2+1} \end{cases} \tag{14}$$

Now, by knowing the distribution of the input and output torques on the sun and the ring, it is possible to derive the dynamic equations for the whole system. The free-body diagram of the system is useful to derive them. Fig. 3 shows the free-body diagrams of the ring and the sun.

According to the free-body diagrams of the sun and the ring, the equations of motion can be easily derived as follows:

$$\begin{cases} T_{in,R} - T_{BR} - T_{out,R} = I_R\dot{\omega}_R \\ T_{in,S} - T_{BS} - T_{out,S} = I_S\dot{\omega}_S \end{cases} \tag{15}$$

Where I_R and I_S are the moments of inertia of the ring and the sun, respectively. T_{BR} and T_{BS} are the braking torques applied to the ring and the sun. When the braking surfaces are slipping the brake torques can be found as:

$$\begin{cases} T_{BR} = -C_R(\mu_R, A_R, r_R)N_{BR}sign(\omega_R) \\ T_{BS} = -C_S(\mu_S, A_S, r_S)N_{BS}sign(\omega_S) \end{cases} \tag{16}$$

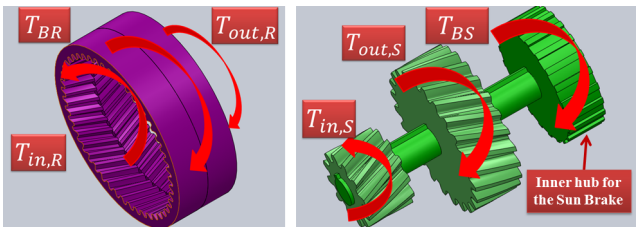

Fig. 3. Free body diagram of the sun and the ring

Where C_R and C_S are the constants of friction for the ring and the sun brakes which are functions of μ, A and r, where μ is the coefficient of friction, A is the effective friction area and r is the effective friction radius. N_{BR} and N_{BS} are the normal brake forces. From equations (14) and (15) it can be easily concluded that:

$$\begin{cases} \dfrac{T_{in,T}R_1}{R_1+1} - T_{BR} - \dfrac{T_{out,T}R_2}{R_2+1} = I_R\dot{\omega}_R \\ \dfrac{T_{in,T}}{R_1+1} - T_{BS} - \dfrac{T_{out,T}}{R_2+1} = I_S\dot{\omega}_S \end{cases} \tag{17}$$

For the electric motor connected to the input carrier and for the load connected to the output carrier, the equations of motion are considered as:

$$\begin{cases} T_{EM} - T_{in,T} = I_M\dot{\omega}_M \\ T_{out,T} - T_{Load} = I_L\dot{\omega}_L \end{cases} \tag{18}$$

Where T_{EM} is the electromagnetic torque of the electric motor. T_{Load} is the load which is exerted to the output carrier. I_M and I_L are the moments of inertia of the motor and the load. It is obvious that $\omega_M = \omega_{in,T}$ and $\omega_L = \omega_{out,T}$. By eliminating the $T_{in,T}$ and $T_{out,T}$ from the equations (17) and (18) and also from the equations (6) and (7), the equations of the motion of the system can be found. During shifting, the two-speed transmission has 2 degrees of freedom but there are 4 speeds available which are dependent (ω_R, ω_S, $\omega_{in,T}$ and $\omega_{out,T}$). It is needed to select two of them to derive the equations of motion. Here, two different points of view are selected to obtain these equations as below:

$$\begin{cases} \dfrac{T_{EM}(R_1d-b)}{R_1+1} - T_{BR}d + T_{BS}b - \dfrac{T_{Load}(R_2d-b)}{R_2+1} = (ad-bc)\dot{\omega}_M \\ \dfrac{T_{EM}(R_1c-a)}{R_1+1} - T_{BR}c + T_{BS}a - \dfrac{T_{Load}(R_2c-a)}{R_2+1} = (bc-ad)\dot{\omega}_L \end{cases} \tag{19}$$

$$\begin{cases} a = (I_R(\dfrac{R_1+1}{R_1-R_2}) + I_M(\dfrac{R_1}{R_1+1})) \\ b = (I_L(\dfrac{R_2}{R_2+1}) - I_R(\dfrac{R_2+1}{R_1-R_2})) \\ c = (I_SR_2(\dfrac{R_1+1}{R_2-R_1}) + I_M(\dfrac{1}{R_1+1})) \\ d = (I_L(\dfrac{1}{R_2+1}) - I_SR_1(\dfrac{R_2+1}{R_2-R_1})) \end{cases}$$

$$\begin{cases} \dfrac{T_{EM}(R_1g-f)}{R_1+1} - T_{BR}g + T_{BS}f - \dfrac{T_{Load}(R_2g-f)}{R_2+1} = (eg-f^2)\dot{\omega}_R \\ \dfrac{T_{EM}(R_1f-e)}{R_1+1} - T_{BR}f + T_{BS}e - \dfrac{T_{Load}(R_2f-e)}{R_2+1} = (f^2-eg)\dot{\omega}_S \end{cases} \tag{20}$$

$$\begin{cases} e = (I_R + I_M(\dfrac{R_1}{R_1+1})^2 + I_L(\dfrac{R_2}{R_2+1})^2) \\ f = I_M(\dfrac{R_1}{(R_1+1)^2}) + I_L(\dfrac{R_2}{(R_2+1)^2}) \\ g = (I_S + I_M(\dfrac{1}{(R_1+1)^2}) + I_L(\dfrac{1}{(R_2+1)^2})) \end{cases}$$

The first sets of equations (19) considers ω_M and ω_L and the second one (20) considers ω_R and ω_S as the dynamic variables.

IV. CONTROL ALGORITHM

In this section, the control scheme for upshift is investigated and the controllers are designed based on it. The scheme consists of two phases, the torque phase and the inertia phase. In the torque phase, the normal brake forces will be controlled and the brakes are switched. At the beginning of the torque phase, the off-going brake is completely engaged and the on-going brake is completely released and at the end of the torque phase, the off-going brake is completely released and the on-going brake is slipping. By looking deeply into the dynamic equations of the system, it can be concluded that by releasing the two brakes, the power will not transfer through the transmission and the input power rotates the ring and the sun in opposite directions. Hence, it is needed to avoid this reverse rotation to transfer the power. There are two ways of doing this. The first is to use a one-way clutch and control it mechanically. The second way is to use the mentioned brakes to control the speeds of the sun and the ring. To control torque by the brakes, at the beginning of the torque phase, a slip controller is activated on the ring brake. This controller should limit the ring not to rotate more than -5 rad/s (the desired speed is considered a negative number very close to zero and not zero to avoid the vibration causes by slip-stick switching)[12]. When the slip controller is activated, the normal brake force of the sun is ramped up. Ramping up the normal brake force of the sun will decreases the required normal brake force of the ring brake. This is because, increasing the normal brake force of the sun will exert positive torque on the ring gear and the normal force of the ring brake should be decreased to compensate. Ramping up the normal brake force of the sun should be up to the point that the slip controller of the ring be deactivated ($N_{BR} = 0$) which is the end of the torque phase. In the next phase, which is the inertia phase, the speed of the motor will be matched with the speed of the driveline in the second gear. At the same time, the output speed and torque of the transmission is controlled by the normal brake force of the sun gear. At the end of the inertia phase, the sun is grounded. During the torque phase, the angular speeds of the ring and the motor need to be controlled. The speed of the motor will be controlled by a PID controller. The input error of the PID controller is the difference between the desired motor speed and the speed of the motor ($e(t) = \omega_{Mdes}(t) - \omega_M(t)$) and output of the PID controller is the required electromagnetic torque of the motor T_{EM}. To find the slip controller for the ring, the first equation in (20) can be rewritten as:

$$\dot{\omega}_R = \frac{\frac{T_{EM}(R_1 g - f)}{R_1+1} - T_{BR} g + T_{BS} f - \frac{T_{Load}(R_2 g - f)}{R_2+1}}{eg - f^2} \tag{21}$$

For the simplification of (21), all the other terms except T_{BR} is considered as T_R like below:

$$T_R = \frac{\frac{T_{EM}(R_1 g - f)}{R_1+1} + T_{BS} f - \frac{T_{Load}(R_2 g - f)}{R_2+1}}{-g} \tag{22}$$

Hence, equation (21) can be rewritten as:

$$\dot{\omega}_R = \frac{T_R + T_{BR}}{\frac{f^2}{g} - e} \tag{23}$$

In the equation (22), T_{EM} is known as it is controlled by the PID controller. T_{BS} is also known because during the torque phase, it is ramped up with a pre-defined slope. The load torque is assumed as a linear function of output speed $T_{Load} = K_L \omega_L$ where K_L is the load constant. Hence, the slip controller of the ring can be found from the input-output feedback linearization method. If the output is considered as:

$$y(t) = \omega_R(t) \tag{24}$$

Then

$$\dot{y}(t) = \dot{\omega}_R(t) = \frac{T_R + T_{BR}}{\frac{f^2}{g} - e} \tag{25}$$

By choosing $T_{BR} = (-T_R + \frac{\nu}{\frac{f^2}{g} - e})$ it can be concluded that $\dot{y}(t) = \nu$. For asymptotically stabilizing the output, the input ν can be chosen as:

$$\nu = \dot{y}_{des}(t) + K_{BR}(y_{des} - y) \tag{26}$$

Where y_{des} is the desired output speed and here it is considered to be constant during the gear shift ($\dot{y}_{des}(t) = 0$). By choosing $K_{BR} = \frac{g}{f^2 - eg}$ then:

$$T_{BR} = (-T_R + (\omega_R(t) - \omega_{Rdes}(t))) \tag{27}$$

Which is the required braking torque to control the speed of the ring gear during the torque phase. The input-output feedback linearization controller just ensures the stability of the output (ω_R) and not the internal stability. As the system has two degree of freedom during the gear shifting, another state needs to be controlled as well. So, the parameters of the PID controller, which was mentioned before, should be tuned to control ω_M by using T_{EM} to obtain the internal stability. Here, the parameters of the PID controller are chosen as $K_P = 50, K_I = 20, K_D = 0$.

For the inertia phase, an optimal H_∞ controller is designed to control the speed of the motor and also output speed. According to the equation sets (19) and because the load torque is considered as a linear function of output speed, then the whole system would be linear.

Now, by considering the state space equation as:

$$\begin{cases} \Delta\dot{X}(t) = A\Delta X(t) + B\Delta U(t) \\ \Delta Y(t) = C\Delta X(t) + D\Delta U(t) \end{cases} \tag{28}$$

$$\Delta X(t) = \begin{bmatrix} \theta_M(t) - \theta_M^*(t) \\ \dot{\theta}_M(t) - \dot{\theta}_M^*(t) \\ \theta_L(t) - \theta_L^*(t) \\ \dot{\theta}_L(t) - \dot{\theta}_L^*(t) \end{bmatrix} = \begin{bmatrix} \theta_M(t) - \theta_M^*(t) \\ \omega_M(t) - \omega_M^*(t) \\ \theta_L(t) - \theta_L^*(t) \\ \omega_L(t) - \omega_L^*(t) \end{bmatrix}$$

$$\Delta U(t) = U(t) - U^*(t) = \begin{bmatrix} \Delta T_{EM} \\ \Delta T_{BS} \end{bmatrix}$$

Where θ_M, θ_L, $\dot{\theta}_M$ and $\dot{\theta}_L$ are the angular position and velocity of the input and output of the transmission and θ_M^*, $\dot{\theta}_M^*$, θ_L^* and $\dot{\theta}_L^*$ and U^* are the initial states and the control input at the beginning of the inertia phase.

By substituting the following parameters of the system in equations (19) and (28):

$$R_1 = 2; R_2 = 4; K_L = 1; C_R = C_S = 0.1;$$
$$I_M = 0.1(Kg.m^2); I_R = 0.001(Kg.m^2)$$
$$I_S = 0.0005(Kg.m^2); I_L = 1.25(Kg.m^2)$$

The A,B,C and D matrices can be obtained as:

$$A = \begin{bmatrix} 0 & 1 & 0 & 0 \\ 0 & 0 & 0 & -0.1232 \\ 0 & 0 & 0 & 1 \\ 0 & 0 & 0 & -0.79 \end{bmatrix} \quad B = \begin{bmatrix} 0 & 0 \\ 8.3352 & -49.3954 \\ 0 & 0 \\ 0.1232 & 3.2109 \end{bmatrix}$$
$$C = \begin{bmatrix} 0 & 1 & 0 & 0 \\ 0 & 0 & 0 & 1 \end{bmatrix} \quad D = \begin{bmatrix} 0 & 0 \\ 0 & 0 \end{bmatrix}$$

These state-space matrices are used to find the transfer function between two inputs (motor torque and sun brake torque) and two outputs (motor and load speeds) of the system. This transfer function can be expressed as:

$$G(s) = \begin{bmatrix} \frac{8.335s+6.57}{s^2+0.79s} & \frac{-49.4s-39.42}{s^2+0.79s} \\ \frac{0.1232}{s^2+0.79s} & \frac{3.211}{s^2+0.79s} \end{bmatrix}$$

When the transfer function of the system is available, it is possible to define weighting function and generalized plant $P(s)$ to design an optimal H_∞ controller. The Fig. 4 shows the generalized plant $P(s)$, the weighting functions $W_u(s)$ and $W_e(s)$ and the normalized input $\Delta\widetilde{u}(s)$ and output $\widetilde{e}(s)$ which are chosen for this purpose. So, the matrix of the generalized plant can be expressed as:

$$\begin{bmatrix} \Delta\widetilde{u}(s) \\ \widetilde{e}(s) \\ e(s) \end{bmatrix} = \overbrace{\begin{bmatrix} 0_{2\times2} & W_u(s) \\ W_e(s) & -W_e(s)G(s) \\ I_{2\times2} & -G(s) \end{bmatrix}}^{P(s)} \begin{bmatrix} \Delta Y_{des}(s) \\ \Delta u(s) \end{bmatrix} \quad (29)$$

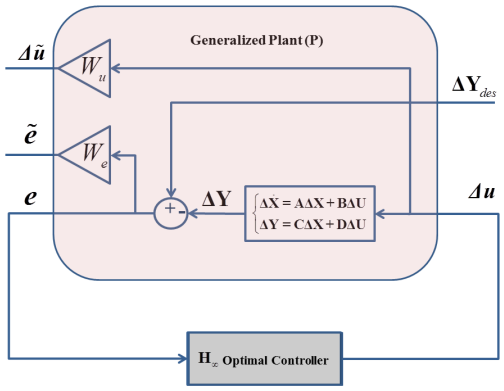

Fig. 4. Generalized plant and weighting functions

where the weighting functions are considered as:

$$W_e(s) = \frac{11}{35s+1}\begin{bmatrix} 1 & 0 \\ 0 & 1 \end{bmatrix}, \quad W_u(s) = \begin{bmatrix} 0.01 & 0 \\ 0 & 9 \end{bmatrix}$$

The reason why the weighting function of T_{BS} is chosen to be so much larger than the weighting function of T_{EM} is to reduce the oscillation of the control input related to the torque brake of the sun and put most of the control responsibility on the electric motor. By using the "hinfsyn" command in MATLAB the controller K and the performance level γ of the H_∞ controller are found as below:

$$K(s) = \begin{bmatrix} K_{11} & K_{12} \\ K_{21} & K_{22} \end{bmatrix}, \quad \gamma = 0.9083.$$

$$\begin{cases} K_{11}(s) = \frac{30.6605s(s+29.9)(s+1.171)}{(s+29.16)(s+23.15)(s+1.252)(s+0.02857)} \\ K_{12}(s) = \frac{33.1783s(s+12.69)(s+0.8051)}{(s+29.16)(s+23.15)(s+1.252)(s+0.02857)} \\ K_{21}(s) = \frac{-0.04981s(s^2+23.75s+279.8)}{(s+29.16)(s+23.15)(s+1.252)(s+0.02857)} \\ K_{22}(s) = \frac{2.9785s(s+22.81)(s+0.7857)}{(s+29.16)(s+23.15)(s+1.252)(s+0.02857)} \end{cases}$$

As γ is less than 1, the desired performance of the closed-loop system is achieved. To validate that, the sensitivity function $S(s) = \frac{1}{1+K(s)G(s)}$ needs to satisfy the following inequality to achieve the desired performance:

$$|S(j\omega)| \leq |W_e^{-1}(j\omega)|, \forall\omega.$$

Where the satisfaction of this inequality can be seen in Fig. 5.

V. SIMULATION RESULTS

In this section, the simulation results for the upshift are provided. The goal of the control is to keep the output speed and torque constant during this process. For the upshift, the speed of the motor needs to decrease to match with the speed of the driveline in the second gear. The simulation results are illustrated in figures 6,7 and 8. Fig. 6 shows the angular velocity of the ring, sun, input and output of the transmission. Fig. 7 shows the input (electric motor) and output (load) torques and Fig. 8 shows the normal braking

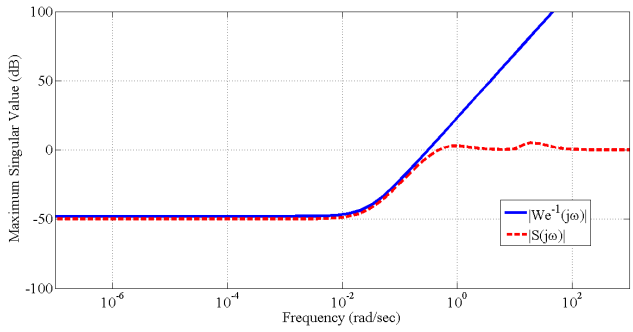

Fig. 5. Maximum Sigular Values of ${W_e}^{-1}(s)$ and $S(s)$

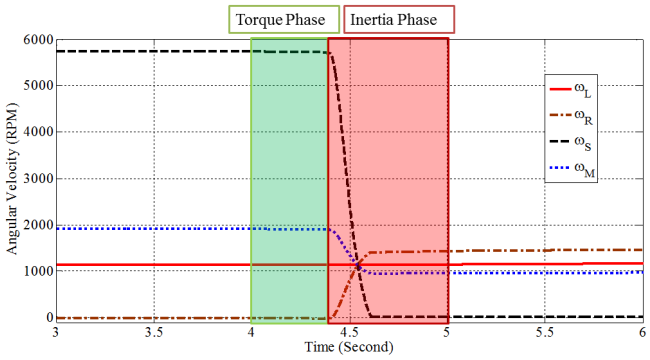

Fig. 6. Angular Velocities of the ω_M, ω_L, ω_R and ω_S (Upshift)

force of the ring and sun brakes during both torque and inertia phases. According to the graphs, the oscillation of the output torque, during the gear change, is about 5 Nm in 90 Nm and the oscillation of the output speed is less than 20 RPM in about 1100 RPM which are not significant. The whole upshift process lasts about 1 second and during this time the output torque and speed remain almost constant which increases the driveability of the vehicle significantly.

VI. CONCLUSION

In this paper, an analytical dynamic model of the proposed two speed automated transmission is presented. The controllers were designed based on the mentioned control algorithm for the upshift and validated by MATLAB/*Simulink*®. The simulation results show that the oscillation of the output torque, during the gear change, is not more than 10% in about 90 Nm, which is negligible. The two embedded brake systems in the proposed transmission not only provide seamless gearshifts, but also help in the synchronization of the speed of the motor with the driveline which can reduce the shifting time. It can be easily shown that the control algorithm for the downshift can be obtained in a similar way to the upshift, the main difference being in the sequence of the inertia and torque phases.

Future work will be validating the proposed modeling and control algorithm on the real testbed and improve the controller to a robust H_∞ optimal one to cover possible uncertainties, disturbances and noise.

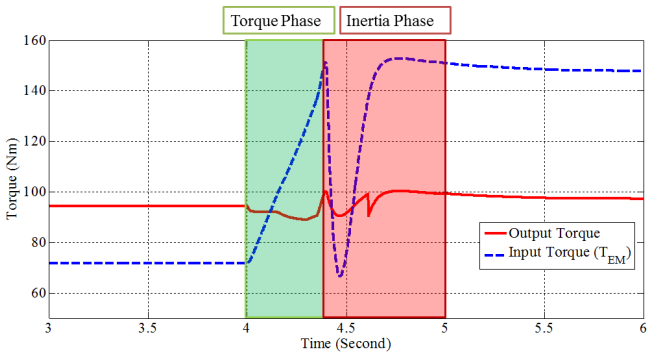

Fig. 7. Input torque and output torque (Upshift)

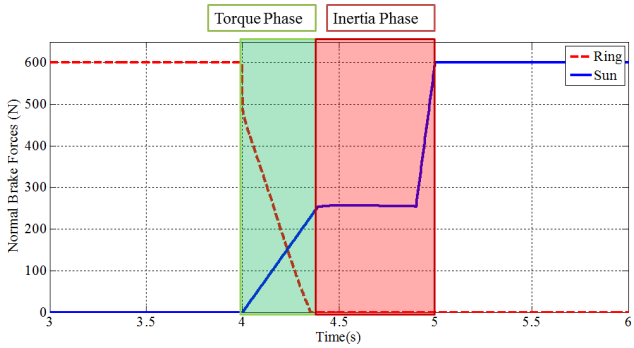

Fig. 8. Normal brake forces of the ring and the sun (Upshift)

VII. ACKNOWLEDGMENT

We gratefully acknowledge the support of our industrial partners: Linamar, TM4 and Infolytica, and the valuable suggestions of Mr. Hossein Vahid Alizadeh to develop the dynamic model of the proposed mechanism.

REFERENCES

[1] X. Y. Song, Z. X. Sun, X. J. Yang and G. M. Zhu, Modelling, control, and hardware-in-the-loop simulation of an automated manual transmission, *IMechE Automobile Eng. J.* vol. 224, Part D, pp. 143-159, Feb 2010.

[2] M. Kulkarni, T. Shim, Y. Zhang, Shift dynamics and control of dual-clutch transmissions, *Mechanism and Machine Theory J., Elsevier*, vol. 42, pp. 168182, May 2006.

[3] P. D. Walker, N. Zhang and R. Tamba, Control of gear shifts in dual clutch transmission powertrains, *Mechanical Systems and Signal J., Elsevier*, vol. 25, pp. 1923-1936, Sept 2010.

[4] J. Kim, K. Cho, and S. B. Choi, Gear Shift Control of Dual Clutch Transmissions with a Torque Rate Limitation Trajectory, *American Control Conf.*, San Francisco, June 2011, pp. 3338-3343.

[5] E. Galvagno, M. Velardocchia and A. Vigliani, Dynamic and kinematic model of a dual clutch transmission, *Mechanism and Machine Theory J. Elsevier*, vol. 46, pp. 794-805, Feb 2011.

[6] N. Srivastava, I. Haque, A review on belt and chain continuously variable transmissions (CVT): Dynamics and control, *Mechanism and Machine Theory J.*, vol. 44, pp. 19-41, August 2008.

[7] Z. Zou, Y. Zhang, X. Zhang and W. Tobler, Modeling and Simulation of Traction Drive Dynamics and Control, *Mechanical Design J. Trans of the ASME*, vol.123, pp. 556-561, Dec 2001.

[8] C. H. Zheng, W. S. Lim and S. W. Cha, Performance Optimization of CVT for Two-Wheeled Vehicles, *Int. J. of Automotive Tech.*, vol. 12, no. 3, pp. 461-468, 2011.

[9] R. Pfiffner and L. Guzzella, Optimal operation of CVT-based powertrains, *Int. J. Robust and Nonlinear Control, John Wiley & Sons*, vol. 11, pp. 1003-1021, 2001.

[10] L. Glielmo, L. Iannelli, V. Vacca, and F. Vasca, Gearshift Control for Automated Manual Transmissions, *IEEE/ASME Trans. Mechatronics*, vol. 11, no. 1, pp. 17-26, Feb 2006.

[11] Y-S Zhao, Z-F Liu, L-G Cai, W-T Yang, J Yang, and Z Luo, Study of control for the automated clutch of an automated manual transmission vehicle based on rapid control prototyping, *J. Automobile Engineering*, part D, vol. 224, pp. 475-487, 2010.

[12] M. Goetz, M. C. Levesley, and D. A. Crolla, Dynamics and control of gearshifts on twin-clutch transmissions, *J. Automobile Engineering*, Part D, vol. 219, pp. 951-963, 2005.

[13] Y. Liu, D. Qin, H. Jiang and Y. Zhang, A Systematic Model for Dynamics and Control of Dual Clutch Transmissions, *J. Mechanical Design*, vol. 131, pp. 1-7, 2009.

[14] P. D. Walker, N. Zhang, Modelling of dual clutch transmission equipped powertrains for shift transient simulations, *Mechanism and Machine Theory J.*, vol 60, pp. 47-59, 2003.

[15] M. C. Tsai, C. C. Huang, B. J. Lin, Kinematic Analysis of Planetary Gear Systems Using Block Diagrams, *J. Mechanical Design*, vol. 132, pp. 1-10, June 2010.